

Phenomenological model of melting in Lennard-Jones clusters

I. L. Garzón and M. Avalos Borja

*Instituto de Física, Universidad Nacional Autónoma de México, Apartado Postal 2681,
22800 Ensenada, Baja California, Mexico*

Estela Blaisten-Barojas*

Surface Science Division, National Institute of Standards and Technology, Gaithersburg, Maryland 20899

(Received 16 March 1989)

Extensive molecular-dynamics simulations were coupled to infinitely fast quenches by steepest descent in order to obtain more information on the melting transition of small clusters with 12 to 14 atoms interacting via Lennard-Jones potentials. A procedure is devised to measure the fraction of times f that the high-energy local minima of the potential-energy surface are accessed during a long trajectory. The computer experiment shows that f depends on temperature and presents a sigmoid shape. The temperature at which f is valued, $\frac{1}{2}$ is identified with the cluster melting temperature T_m . This is a new criterion that can be framed into a phenomenological description of melting in clusters. The theoretical model is based on a mapping of the segments of a copolymer with the short-time excursions of the cluster among the high-energy local minima. Melting in this pseudopolymer is characterized by the S -shaped behavior of f as a function of temperature. In small clusters the slope of f at T_m is moderately high, the width of the transition region being $\approx 0.3T_m$. The 12- and 13-atom clusters melt at 0.24ϵ and 0.3ϵ . The 14-atom cluster evaporates before melting.

I. INTRODUCTION

Considerable attention has been paid recently to provide extended simulation studies of melting in clusters containing very few atoms.¹⁻⁴ Although the melting transition in Lennard-Jones clusters was studied years ago,¹ many features are not yet understood. Recent molecular-dynamics simulations²⁻⁴ have shown that long-time averages are needed in order to compensate for the large thermodynamic fluctuations characteristic of systems with a few atoms. The main concern is to provide more support to describe "melting" other than the behavior of the cluster energy as a function of temperature. For clusters it is usual to identify melting in a computer simulation when this dependence gives rise to a loop-shaped curve. This is not always the case.⁵ For various cluster sizes,² or other model potentials,⁴ no loop is apparent. The identification of a melting transition from the E versus T curve is obscured because the thermodynamic states (points on this curve) contain the distracting contribution of vibrations.

Melting in finite systems other than clusters is commonly described in terms of a property that changes abruptly with temperature between two extreme values. A typical example is the helix-coil transition observed in certain polymers with helical structure.^{6,7} The Ising model and related models have been applied with success to a number of finite systems such as polymers and biological molecules.^{8,9} In particular, Poland and Scheraga have discussed along these lines a certain number of processes related to melting of biological molecules using the Ising-model language. An example is the denaturation process in DNA. Saturation in allosteric enzymes and oxygenation of hemoglobin have also been treated with

various decorated Ising models.⁹

For clusters, an approach to the description of melting has been formulated on the basis of a two-state model³ as a solidlike cluster undergoing a chemical equilibrium change into a liquidlike cluster. Jellinek *et al.*² have characterized this change by the observation in molecular-dynamics simulations of a bimodal distribution of short-time-averaged kinetic energies in the melting temperature region. In that range of temperatures, the high-temperature form is associated with the rigid, solidlike cluster, and the low-temperature form displays the properties of a nonrigid, liquidlike cluster. This approach relies on the study of the temperature (average kinetic energy) fluctuations. In earlier works for the 13-atom cluster, Honeycutt and Andersen,³ and the authors of this paper,⁴ have stated that a meltinglike transition could be interpreted as the change with temperature from the icosahedron (solidlike phase) to a "set" of isomeric high-energy structures (liquidlike phase). Here the disordered state is associated with the way the system packs its atoms during its time evolution in phase space. The changes between various packings are evident in a molecular-dynamics simulation after drawing the cluster configurations as time evolves along the trajectory at a fixed energy. In this work we provide a procedure for computer measurements of these observations and also we restate the two-state model under the Ising-model language used for polymers.

The central idea is to extract the inherent structural part from the vibrational part of an ordered state.¹⁰ To accomplish this goal we describe the computer experiment that measures the inherent structure of the 13-atom cluster in Sec. II. This configurational inspection is generated by quenches following the steepest descent paths

on the potential-energy hypersurface.¹⁰ First, we generate the curve of total energy E as a function of temperature T . Second, for nine different thermodynamic states we propagate the system for 30 000 extra time steps. This procedure yields a good average value of the kinetic energy. Third, we collect the distribution of underlying local minima during another 90 000 steps for six of those thermodynamic steps. This allows us to record the frequency with which the cluster “visits” the global minimum (icosahedron) or any of the multitude of local minima. Thus, we can account for the fraction of times, f , that minima other than the icosahedron are accessed during the trajectory. This quantity, f , changes from zero at low temperatures to one at high temperatures and presents a sigmoid shape in between. We propose to associate melting in clusters with the measure of f as a function of temperature. Therefore, we identify the temperature where f is valued $\frac{1}{2}$ as the melting temperature of the cluster. We propose this novel criterion as an alternative to other criteria,^{11,12} which are mainly based on observations of the bulk material. The second part of this work, which is described in Sec. III, is dedicated to presenting a theoretical treatment of melting, based on a mapping of the excursions of the cluster between the global and local minima along a path in configuration space, with a polymer containing n binding units and all nearest-neighbor interactions. Formally, this is obtained by working out the dynamics of a one-dimensional correlated walk⁷ with two states. This treatment gives better results than the Zimm and Bragg^{6,8} model of the helix-coil transition in α -helix polypeptides. Within this model, f , the fraction of times the cluster accesses minima, other than the icosahedron along a path in configuration space, can be calculated exactly. The theoretical treatment contains two parameters, which can be chosen on the basis of the results obtained in the computer experiments. With this model we can discuss a more general classification of clusters as it is given in Sec. IV. Section V of this paper contains several concluding remarks. While the theory offered here is phenomenological, it suggests that the melting process in clusters exhibits a degree of cooperativity between the various high-energy isomeric structures describing the disordered phase, i.e., the access to a particular local minimum favors the access to other local minimum.

II. THE COMPUTER EXPERIMENT

The cluster is defined as an aggregate of $N=12, 13$, or 14 atoms. The interactions between the atoms are represented by pairwise potentials of the Lennard-Jones (LJ) type, such that the total potential energy is

$$V = 4\epsilon \sum_{i < j = 1}^N [(\sigma/r_{ij})^{12} - (\sigma/r_{ij})^6]. \quad (1)$$

The configuration space of these clusters has been extensively studied.^{13–16} It is known that the global minimum of the $3N - 6$ configuration hypersurface is the icosahedron, and that there exist at least 987 more local minima describing other stable isomeric forms.¹⁴ The binding energy of all these isomers gives rise to a distribution $n(V)$, which shows that the icosahedron binding energy is well

detached from its nearest competitors by a gap of 2.85ϵ (see Fig. 16 of Ref. 14). This situation seems ideal for our purposes because of two reasons. First, we refer to a class of clusters for which there exists a well-defined gap ΔV between the binding energy of the most stable isomer and that of all the others. In the icosahedron, the energy of the gap ΔV is roughly the balance which remains after the breaking of the six bonds between the central atom and one of the surface atoms and the formation of three new bonds, which accommodate the atom that pops out. Secondly, we refer to a cluster that has many local minima associated with mechanically stable packings of the N atoms.

Constant energy molecular dynamics was used in this computer experiment. The Newton equations of motion were solved using Verlet’s algorithm¹⁷ with a time step of 0.01τ , where $\tau = (m\sigma^2/\epsilon)^{1/2}$. If the system were argon $\tau = 2.2$ ps. The LJ values of ϵ and $r_0 = 2^{1/6}\sigma$ were adopted as units of energy and distance. Temperature will be reported in reduced units of ϵ/k , where k is Boltzmann’s constant. Reduced units will be quoted with an asterisk (*). The center-of-mass momentum and the total angular momentum of the cluster were eliminated from the calculations. Consequently, temperature refers only to vibrational motions, and was defined as

$$kT = 2 \langle E_{\text{kin}} \rangle / (3N - 6),$$

where $\langle E_{\text{kin}} \rangle$ is the time-averaged kinetic energy of the cluster.

The first step in this simulation was to generate the curve of total energy per particle as a function of temperature.^{1–4} The resulting equilibrium thermodynamic states (points on the curve) are reported in Figs. 1(a) and 1(b). The experiment was started from a cold cluster in the geometry corresponding to the global minimum. Each state was allowed to run for 130τ . During each run, 30τ were allowed for equilibration, and open circles on Fig. 1(a) correspond to averages on the remainder 100τ . At the end of this time interval, the velocities were scaled by a factor 1.1. This is a steplike heating process that simulates a heating rate $\Delta T/\Delta t$ of 10 K/ns in the case of argon. An external thermal energy of 0.4ϵ is given to the system in 2200τ . No constraint was imposed on the total energy in going from one heating step to the next. Consequently, the energy should be constant within each heating step, although it may change in going from one to the other heating steps. Furthermore, we have tested that in each heating step the temperature fluctuations became constant after the first 30τ , i.e., $\sigma_T \approx 1/(3N - 6)^{1/2}$ this provided us with a criterion for equilibrium.

Despite this fact, we propagated the system for 30 000 extra time steps, in the temperature region where the transition temperature was suspected to occur. Therefore, the solid circles in Figs. 1(a) and 1(b) correspond to averages over 330τ . In Figs. 1(a) and 1(b) we show a process in which the system distributed the kinetic energy equally among the $3N - 6$ degrees of freedom. This can be measured by the slope at low temperatures of the E versus T curve. In reaching the S-shaped region of the curve, the system is hot enough as to allow for the first

group of bonds between one of the surface atoms and the central atom to break. In doing so, it starts a trajectory in configuration space that takes it to "visit" a set of isomeric structures. The concept of visit will be made clear below.

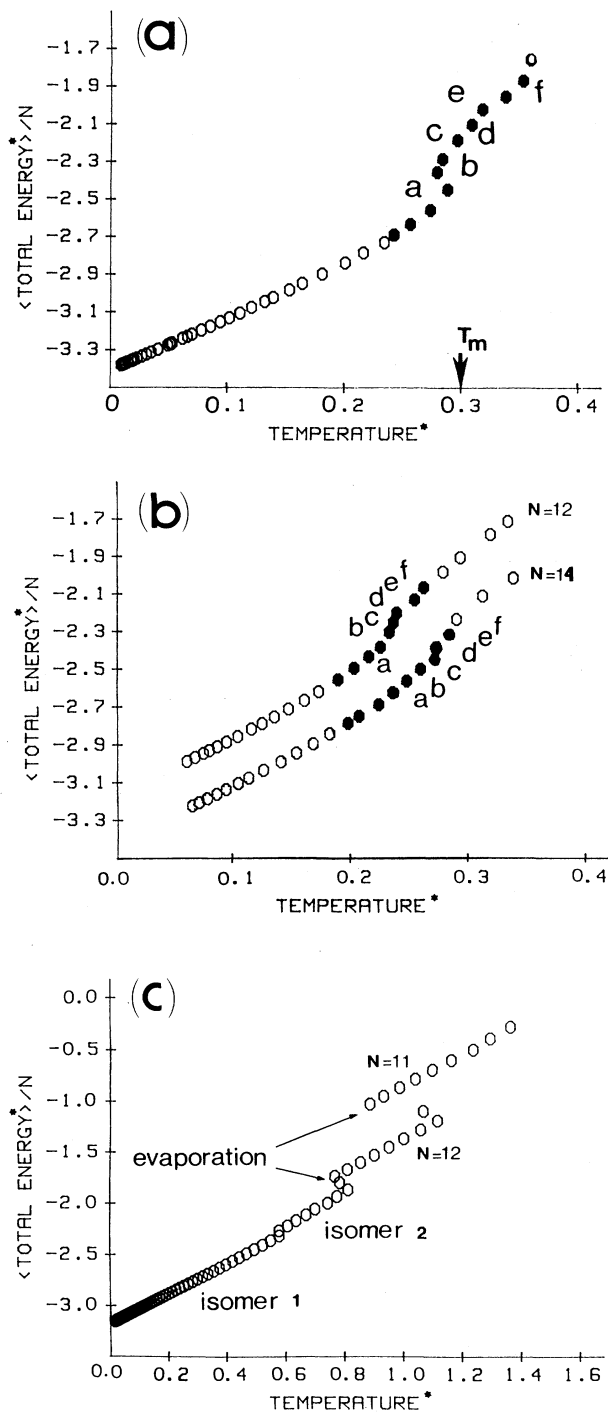


FIG. 1. Total energy as a function of temperature in reduced units. (a) $N=13$. The melting temperature is indicated as T_m . (b) $N=12$ (○) and $N=14$ (○). (c) Slow heating rate experiment starting from the first isomer of the 13-atom cluster.

Faster heating processes drive the system into metastable states too rapidly, and evaporation follows. With slower heating rates it is possible to keep the system in metastable regions during observable times. In Fig. 1(c) we give the result obtained when the heating process is initiated from the 13-atom isomer with lowest potential energy above the icosahedron, i.e., -3.190ϵ .¹⁴⁻¹⁶ Since this is a metastable state, heating too fast produces evaporation of one atom. Thus, in this case the velocities were scaled by a factor 1.03, and each point on the curve corresponds to an average over 300τ . The first jump in Fig. 1(c) depicts a change into a second isomeric form, with potential energy equal to 3.184ϵ .¹⁶ The system needs to be very hot ($kT=0.6\epsilon$) before undergoing a change of packing. In the second jump there is evaporation of one atom, and finally in the third jump, a second atom evaporates. It is interesting to point out that the single stripping of an atom is followed by a lowering in the temperature of the system. Therefore, the system cools while it evaporates one atom. This effect was observed in all of our experiments.

In order to better understand the differences between the lowest-energy isomers in the 13-atom cluster, we calculated the frequency distribution of the normal modes for the icosahedron (nine degenerate modes) and for the three isomeric structures above the gap with energies -3.190ϵ , -3.184ϵ , and -3.128ϵ . These are shown in Fig. 2. Each normal frequency has been depicted by a δ function whose height measures the degeneracy of the mode. There are several interesting features: First, the width of the band does not change much with the isomer. The cutoff frequency is approximately $25\tau^{-1}$ in all cases.

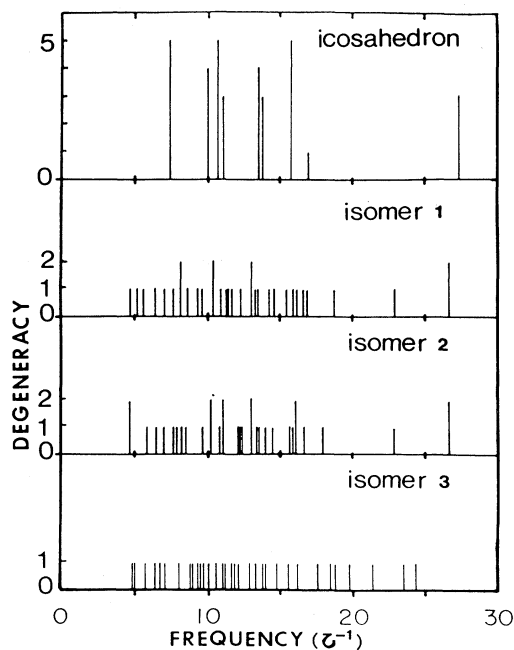


FIG. 2. Normal mode frequencies of the icosahedron and three 13-atom isomers above the gap ΔV .

Low frequencies are absent from the distribution. Second, the degeneracy of the modes disappears when the icosahedral symmetry is broken. Third, the distribution of frequencies pertain to the array of 13 atoms as a whole and not to a repetitive unit within the cluster. Fourth, all these collective frequencies are much higher than the characteristic frequency of the dimer $\approx 10\tau^{-1}$. The free energy^{18,19} calculated in the harmonic approximation from the normal modes is shown in Fig. 3 for each one of these isomers. The curves are almost parallel at all temperatures. If there had been a crossing between these curves, then the harmonic approximation would have been sufficient to describe melting. This, however, is not the case in the region of temperatures where E versus T presents a hump. It is possible to state, however, that in the classical limit, the harmonic approximation for the entropy difference between the high-energy isomers (HEI) 1–3, and the icosahedron is positive. The structure of the cluster is more disordered in the HEI. Specifically, $\Delta S > 0$ and

$$\begin{aligned} \Delta S &= S_j - S_{\text{ico}} \\ &= \frac{k}{N} \sum_{s=1}^{3N-6} \ln(\omega_s^{\text{ico}} / \omega_s^{(j)}), \quad j=1,2,3, \end{aligned} \quad (2)$$

where ω_s^{ico} , $\omega_s^{(j)}$ are the normal mode frequencies of the icosahedron and the j th HEI, respectively. It is also possible to calculate in this limit, the root-mean-squared displacement of atoms about their equilibrium positions for each isomer. This is given by

$$\langle \delta u^2 \rangle = \frac{3kT}{m} \sum_{s=1}^{3N-6} \frac{1}{\omega_s^2}. \quad (3)$$

The ratios $\langle \delta u^2 \rangle_{\text{ico}} / \langle \delta u^2 \rangle_j$ are 0.755, 0.741, 0.754 for $j=1,2,3$ at any T . It is difficult to say if one or all of these HEI represent the disordered phase. Based on Lindemann's¹¹ rule, i.e., ratio $\langle \delta u^2 \rangle_{\text{ico}} / a^2)^{1/2} \approx 0.25$, the

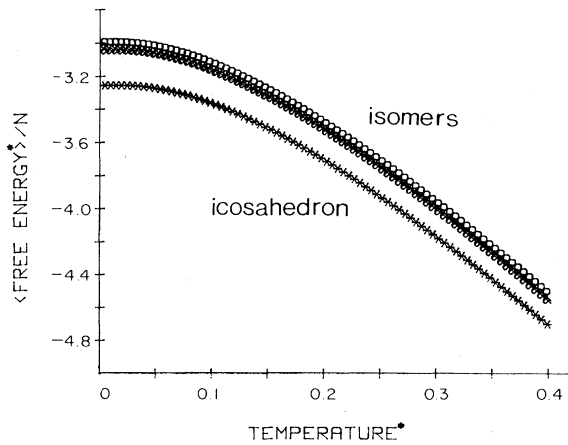


FIG. 3. Free energy per particle for the 13-atom cluster as a function of temperature. Lower line corresponds to the icosahedron. Other lines correspond to the three higher-energy isomers. Reduced units were used.

melting temperature is $T_m^* = 0.23$ when $a = 0.99r_0$ and,

$$\sum_s (\omega_s^{\text{ico}})^{-2} = 0.2688\tau^{-2}.$$

This temperature seems very low. If the same calculation is done for the three HEI, the corresponding “melting” temperature would be ≈ 0.18 . Again this value is very low. Moreover, Fig. 1(c) shows a very smooth curve E versus T at that temperature.

The harmonic analysis, does not seem to give a complete description of melting. Anharmonicities are very important in clusters, as has indirectly been shown² when studying the power spectrum. Besides, the universality of Lindemann's criterion has not been proved to be size independent.

The second stage of the simulation was to identify a fluctuating variable such that its average value would provide a signature of the order (or disorder) in the system. To achieve this goal, each of the points labeled $a-f$ in Figs. 1(a) and 1(b) was propagated for another 900τ . In some states, e.g., state f for $N=12$, states d through f for $N=13$, state f for $N=14$, evaporation took place before 900τ had elapsed. In these cases, we considered shorter trajectories. The molecular-dynamics run was stopped and quenched¹⁰ every 5τ to a local minimum of V . Quenches were achieved by minimizing the potential-energy function with respect to its $3N-6$ variables, i.e., the $3N-6$ internal coordinates. By this means, we generate a mapping from the continuous variable $r(t)$ onto a discrete set of at least 120 minima (240 in some cases) of the potential-energy surface for each temperature. Many of these minima will be repeated because mechanically stable atomic packings will be identical except for particle permutations. Each one of these quenching operations will be called a “visit” to a particular minimum. The number of visits to each minimum in the potential-energy hypersurface were recorded for several temperatures, and plotted in the form of a histogram of binding energies, which changes with temperature. These distributions are depicted in Fig. 4 for the 13-atom cluster and for the six temperatures labeled $a-f$ in Fig. 1(a). At low temperatures the icosahedron (peak at low potential energy) is more frequently visited than the isomers above the gap ΔV [Fig. 4(a)]. As the temperature increases, vibrations allow the cluster to change more easily from one isomeric form into another, resulting in more visits to potential energies above the gap ΔV [Fig. 4(f)]. In other words, the inherent structure of hot clusters is associated with packings corresponding to a set of distinct isomeric structures. Since temperature is the experimental variable, there is a maximum experimental temperature above which evaporation is observed in less than 900τ . We have referred to that maximum temperature as defining an energy threshold for evaporation. This threshold is 0.4ϵ . We found that 44 distinct isomers (out of the 987 known) were visited during the length of the runs. The mean potential-energy spacing in the distribution between any two of these minima contiguous in energy is $1.2 \times 10^{-2}\epsilon/\text{atom}$. We refer to this quantity as δ .

With this experiment we want to convey the idea that a

measure of disorder in the system is related to the concentration of isomeric structures, which lie above the gap ΔV , and which are visited during a reasonably long-time interval. Equivalent runs started from different initial conditions will probably populate several other isomers. In Table I we have gathered the relevant data for the 13-atom cluster. Labeled thermodynamic states refer to the points shown in Fig. 1(a). Each row provides the data obtained from averaging quantities over the time interval shown in column 3. Columns 4–6 give the average potential energy, the temperature and the fraction (f) of minima lying above the gap ΔV , which are visited from a total of n visits. This inherent property changes between zero and almost one in a fairly broad range of temperatures $\Delta T^* \approx 0.09$. The temperature T_m , where f has the value of $\frac{1}{2}$ will be identified as the "melting temperature."

At $T_m^* = 0.3$ the cluster visits the icosahedron and those minima above the gap an equal number of times. This criterion is an alternative approach¹⁻⁴ used to decide when a cluster melts. Furthermore, this new criterion used to locate T_m is independent on the cluster size. The values of T_m obtained in this manner are in agreement with other estimations.^{1-4,20}

In Table II we give the data obtained for the 12- and 14-atom clusters. The 12-atom cluster visited eight different minima with $\Delta V = 0.14\epsilon$ and $\delta = 1.6 \times 10^{-2}\epsilon$. The 14-atom cluster also accessed eight different minima before the evaporation threshold. For this cluster $\Delta V = 0.12\epsilon$ and $\delta = 1.1 \times 10^{-2}\epsilon$. It is clear from the data of Table II that the 14-atom cluster evaporates one atom at low temperatures. Hence, f reaches the value of $\frac{1}{2}$. Evaporation takes place before the cluster effectively

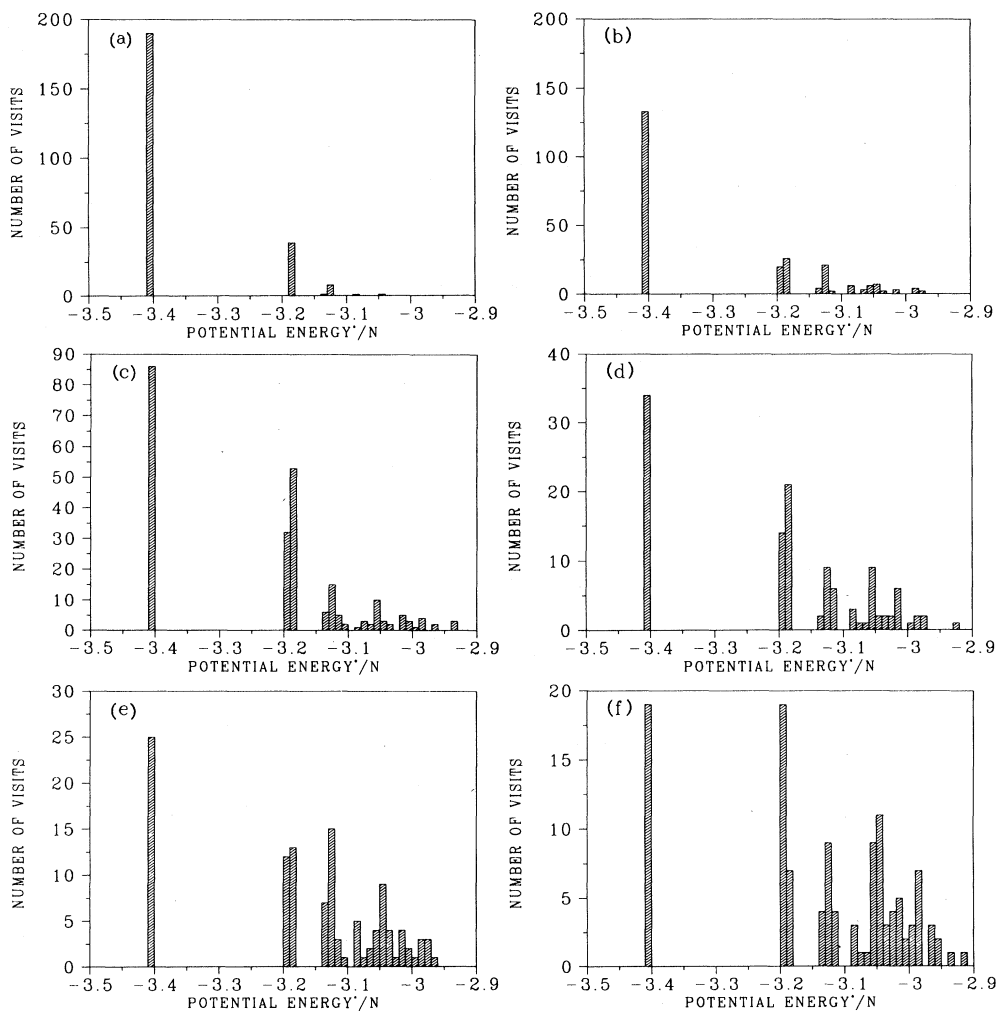


FIG. 4. Histogram of the number of visits to the various minima for the six thermodynamic states labeled $a-f$ in Fig. 1(a). Potential energy is in reduced units.

TABLE I. Total energy per particle, average potential energy, temperatures, and fraction of visits to isomers above the gap for the 13-atom clusters and for runs of various lengths.

State	$\langle E^* \rangle / N$	Run length (τ)	$\langle V^* \rangle / N$	T^*	f
<i>a</i>	-2.4568	300	-2.8240	0.2893	0.17
		600	-2.8110	0.2791	0.26
		900	-2.8130	0.2806	0.22
		1200	-2.8141	0.2815	0.20
<i>b</i>	-2.2938	300	-2.6554	0.2849	0.48
		600	-2.6504	0.2888	0.43
		900	-2.6534	0.2835	0.48
		1200	-2.6578	0.2868	0.45
<i>c</i>	-2.1940	300	-2.5720	0.2978	0.60
		600	-2.5738	0.2993	0.64
		900	-2.5753	0.3004	0.64
		1200	-2.5741	0.2995	0.65
<i>d</i>	-2.1113	300	-2.5048	0.3101	0.72
		600	-2.5046	0.3099	0.72
		900	(evaporation)		
		300	-2.4347	0.3192	0.85
<i>e</i>	-2.0296	600	-2.4375	0.3213	0.79
		900	(evaporation)		
		300	-2.3268	0.3541	0.85
		600	-2.3247	0.3524	0.87
<i>f</i>	-1.8774	900	(evaporation)		

TABLE II. Total energy per particle, average potential energy, temperature, and fraction of visits to isomers above the gap for the 12- and 14-atom clusters.

State	$\langle E^* \rangle / N$	Run length (τ)	$\langle V^* \rangle / N$	T^*	f
<i>N</i> = 12					
<i>a</i>	-2.4441	300	-2.7401	0.2153	0.08
		1200	-2.7340	0.2109	0.14
<i>b</i>	-2.3177	300	-2.6248	0.2330	0.20
		1200	-2.6386	0.2334	0.25
<i>c</i>	-2.2657	300	-2.5910	0.2365	0.45
		1200	-2.5909	0.2365	0.40
<i>d</i>	-2.2156	300	-2.5450	0.2395	0.52
		1200	-2.5464	0.2405	0.54
<i>e</i>	-2.1457	300	-2.4963	0.2550	0.55
		1200	-2.4882	0.2564	0.55
<i>f</i>	-2.0822	300	-2.4434	0.2628	0.72
		600	-2.4468	0.2652	0.62
		900	(evaporation)		
<i>N</i> = 14					
<i>b</i>	-2.5040	300	-2.8662	0.2600	0.05
		1200	-2.8704	0.2631	0.05
<i>c</i>	-2.4487	300	-2.8237	0.2727	0.12
		1200	-2.8271	0.2717	0.12
<i>d</i>	-2.3904	300	-2.7613	0.2741	0.22
		1200	-2.7774	0.2779	0.16
<i>e</i>	-2.3217	300	-2.7306	0.2936	0.33
		900	-2.7211	0.2867	0.28
		1200	(evaporation)		
<i>f</i>	-2.2415	300	(evaporation)		

melts. The cluster cools in the process of evaporation and eventually forms the icosahedron. This observation indicates that the 13-atom fragment is relatively more stable at high temperatures. At these temperatures a dilute mixture of 13- and 14-atom clusters will rapidly give rise to a mixture of isolated atoms and 13-atom clusters. The 12-atom cluster goes through melting at $T_m^* = 0.24$. But since f is valued at only 0.67 when evaporation occurs, the cluster is never really "liquid."

We can contest the fact of having selected arbitrarily a time interval of $t_q = 5\tau$ between quenches. In our case it is very long compared to the periods associated with the softer modes of the 13-atom cluster. As seen from Fig. 2, the softer modes give rise to periods at least 1 order of magnitude smaller than our time interval. The entire cluster has performed at least ten oscillations between two successive quenches. However, in going from one minimum into another, the system necessarily goes through saddles. It is known that classically a system spends long times on the saddle^{21,22} (as the inverse of the speed). Therefore, when the quenches are performed at sufficiently high temperatures, the system will most probably be on a saddle. In this case the cluster will most likely visit the minimum presenting the steepest slope. To investigate this point we have considered the effect of different choices of the quenching time interval t_q . Consider a specific trajectory of 1200τ for the 12- and 13-atom clusters at the temperature where presumably, the system visits with equal probability ($f = \frac{1}{2}$) either the icosahedron (I) or any minimum above ΔV . We will call these minima "broken icosahedra" B . Compute from this trajectory, f as a function of t_q . Compute also the joint frequencies (1) of obtaining the icosahedron immediately after itself (f_{II}), (2) of going into B immediately after obtaining the I icosahedron ($f_{IB} = f_{BI}$), and (3) of visiting two successive B (f_{BB}). As shown in Fig. 5 for the 13-atom cluster, when the chosen time interval t_q is increased, all the joint frequencies tend fairly rapidly towards $\frac{1}{4}$. Therefore, if a trajectory is broken into time

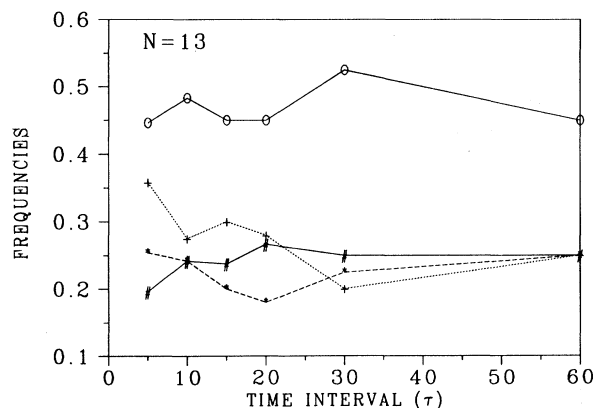


FIG. 5. Joint frequencies as a function of time interval for the 13-atom cluster: f (-o-o-); f_{II} (+...+...); f_{BB} (*- - -*- - -); f_{IB} (#- - - #- - -).

segments, and the state at the end of each segment is analyzed by the steepest descent method, the occurrence of pairs II or BB is favored. Contingent upon $f = 1 - f = \frac{1}{2}$, the system likes to form "dimers;" i.e., $f_{II} = f_{BB} = f_{IB} = f_{BI} = \frac{1}{4}$, at the presumed melting temperature. The choice $t_q = 5\tau$ seems, therefore, quite reasonable since we are close to the limiting value and the effect of this pairing will certainly be accounted for. The same behavior was observed for the 12-atom cluster.

In fact, that $f_{ij} = \frac{1}{4}$, for $i, j = I$ or B , contains more information. Suppose that at T_m the cluster spends all its time on the saddles (or on other complicated topologies of the potential-energy hypersurface) "near" the global minimum. If the slopes leading to all of the minima are similar, the quenching method will drive the system either to I or B with frequency $I - f = f = \frac{1}{2}$, but no dimers will form. In this case $f_{II} = f_{BB} = 0$ and $f_{IB} = f_{BI} = \frac{1}{2}$. Suppose further that the system spends a finite amount of time on the saddles and the rest of the time either on I or B such that $f = \frac{1}{2}$. Then, for similar slopes leading to the closer minima, and for long enough t_q , the joint frequencies will be

$$f_{II} = f_{BB} = f_{IB} = f_{BI} = (1 - f) = \frac{1}{4}.$$

This is what we observe. Therefore, the clusters spend a finite amount of time in regions of configuration space other than the minima wells. At T_m , it seems reasonable to define an average potential barrier as the cluster average potential energy when it is not in a well. Although barriers are quantities which are difficult to measure, we will give an estimate from the considerations to be discussed in Sec. III.

An ideal experiment would be to repeat the analysis of this section many times, generating for each cluster size a set of trajectories with slightly different initial conditions. However, this effort needs a considerable investment of both computer time and storage. We have chosen a different approach described in Sec. III.

We have emphasized on the measure of a quantity like f because it can eventually be observed in the laboratory. Suppose we were able to measure in the laboratory the infrared (ir) or Raman spectra of the 13-atom cluster normal frequencies as a function of their temperature. It would be possible to detect how the integrated intensity of the normal modes decrease with temperature. These intensities would be proportional to f .

III. MELTING BASED ON A CORRELATED WALK MODEL

Certain features of the cluster potential-energy hypersurface can be used to define a class of clusters when they are observed. These are the following.

- (1) The presence of many mechanically stable isomeric packings associated with local minima of the potential energy.
- (2) The existence of a potential-energy gap in the distribution $[n(V)]$ of potential energies associated with those minima. The gap separates one (or eventually a few) isomeric packing at low energies from all the others at

high energies.

(3) The requirement that δ , the mean nearest-neighbor energy spacing between potential energies of the isomers above the gap, be considerably smaller than ΔV .

The 12-, 13-, and 14-atom Lennard-Jones clusters belong to this class. The icosahedron is well detached in potential energy by 0.22ϵ /atom from the other stable isomers, 44 stable isomers were detected dynamically below the evaporation threshold, and δ_{13} was found to be $1.2 \times 10^{-2} \epsilon$ /atom. The 12- and 14-atom clusters both have fairly large gaps as compared to $\delta(\Delta V_{12}=0.14\epsilon, \delta_{12}=1.6 \times 10^{-2}\epsilon, \Delta V_{14}=0.12\epsilon, \delta_{14}=1.1 \times 10^{-2})$. In both cases, however, the number of minima which were located before evaporation occurred was small. Evaporation and melting are therefore competing. This is clear from the values of f in Table II.

In the previous section we discussed an experiment in which a trajectory 1200τ long (600 long for some states) was split into short-time segments $t_q=5\tau$. At the end of each of these segments an infinitely fast quench drove the system to a minimum of the potential-energy hypersurface. Therefore, for each thermodynamic state considered, we have n visits to an equal number of minima. These minima can be visited more than once as was shown in Fig. 4. The result of these operations is a string of n symbols $IBBBIIIBIBIB \dots n$. We propose to map the trajectory onto one state of a one-dimensional walker. This walker steps n times on these minima, each step having two probabilities of arrival p_I and p_B . These probabilities are characterized by two different energy states of the cluster; e_I and e_B . The energy difference $e_B - e_I$ is at least ΔV . An ensemble of trajectories, prepared from a convenient set of initial conditions, then maps onto the ensemble of states of the walker. Furthermore, we propose that two contiguous steps are correlated, but that no correlation exists between steps further apart. Therefore we assume that the probability distribution of states of the walker is Markovian. The recipe for constructing the probability of one state of the walker,^{7,8} and therefore its weight to the canonical partition function, is I after I weights 1, B after B weights $p_B/p_I = \phi$, B after I weights $\psi\phi$, and I after B weights ψ . Let n_B be the number of B 's, n_{BI} be the number of junctions between (both types) B 's and I 's, with $n_I = n - n_B$ being the number of I 's. Then we have the number of ϕ 's $= n_B - n_{BI}/2$, the number of 1 's $= n - n_B - n_{BI}/2$, and the number of ψ 's $= n_{BI}/2$. Thus the probability of any one state of the weaker (i.e., string of I 's and B 's) which incorporates the proper nearest-neighbor statistical weights for n_B B 's subject to $n_{BI}/2$ junctions is

$$\phi^{n_B - n_{BI}/2} (\psi^2 \phi)^{n_{BI}/2}. \quad (4)$$

Since there are many ways to rearrange this sequence of B 's and I 's, the partition function is

$$Z = \sum_{n_B} \sum_{n_{BI}} g(n, n_B, n_{BI}) \phi^{n_B} \psi^{n_{BI}}, \quad (5)$$

where $g(n, n_B, n_{BI})$ is a combinatorial factor. The ensemble average values of n_B and n_{BI} are

$$\langle n_B \rangle = \frac{\partial(\ln Z)}{\partial(\ln \phi)}, \quad \langle n_{BI} \rangle = \frac{\partial(\ln Z)}{\partial(\ln \psi)}. \quad (6)$$

It is standard to calculate Z from the two eigenvalues λ_0, λ_1 of the transfer matrix^{8,9}

$$T = \begin{pmatrix} 1 & \psi\phi \\ \psi & \phi \end{pmatrix}, \quad (7)$$

such that $Z = C_0 \lambda_0^n + C_1 \lambda_1^n$. In the limit of large n only the largest eigenvalue λ_0 contributes to Z . Thus, the average fraction of broken icosahedra is given by

$$f = \frac{\langle n_B \rangle}{n} = \frac{\phi}{2\lambda_0} \left[1 + \frac{(\phi-1) + 2\psi^2}{[(1-\phi)^2 + 4^2\phi]^{1/2}} \right]. \quad (8)$$

Our problem is now to give a representation to the probabilities ϕ, ψ , that are related to the cluster trajectories. We propose

$$\begin{aligned} \phi &= \phi_0 e^{-\alpha \Delta V / kT}, \\ \psi &= e^{-K/kT}, \end{aligned} \quad (9)$$

with the condition that at T_m , $\phi=1$, and $\psi=1/4$. The factor ϕ_0 is entropic and depends on the number of minima Ω , all of which were labeled as B 's. The previous conditions lead to

$$\ln \phi_0 = \alpha \frac{\Delta V}{kT_m} = \Omega, \quad (10a)$$

and

$$\frac{K}{kT_m} = \ln 4, \quad (10b)$$

which give a unique value for both α and K . Therefore, the only parameter is T_m . It is difficult to obtain an accurate estimate of Ω . An alternative strategy is to set $\ln \phi = \alpha(T)/kT$, and expand α near T_m subject to the condition $\phi=1$ at T_m ,

$$\alpha(T) = \alpha(T_m) + \alpha' \left[\frac{T}{T_m} - 1 \right] + \dots \quad (11)$$

Since $\alpha(T_m)=0$ we are left with a second parameter, namely α' . Now T_m and α' can be extracted from the molecular-dynamics values of f . From Tables I and II we extract $T_m=0.3\epsilon$ and 0.24ϵ for the 13- and 12-atom clusters. With these values and using Eqs. (10) we obtain $K_{13}=0.42\epsilon$ and $K_{12}=0.33\epsilon$, respectively. Injecting the value of T_m in Eq. (8), and performing a nonlinear fit to the data of f we obtain $\alpha'=7.62\epsilon$ and 5.54ϵ for the 13- and 12-atom clusters. The solid curve in Figs. 6(a) and 6(b) shows the resulting plot of Eq. (8) using the above values of T_m and α' . Circles correspond to the data generated in the computer experiment data, and are reported in Tables I and II. The agreement is excellent.

In general, mappings of the correlated one-dimensional walk, such as is used in biopolymers, lead to an expression for f that depends on ϕ and ψ . T_m is not considered as an independent parameter, but rather it is the temperature (or pH or solvent effect) that constrains ϕ to be 1.

Also, in biopolymers ψ does not usually depend on temperature. Rather, it reflects the fact that the system goes from a state of high local entropy to a state of low local entropy with a very small probability. Usually, for heterogeneous spin systems in a magnetic field that use the Ising model, ψ is set equal to the Boltzmann factor $\exp(-K/kT)$ and K is a paramagnetic energy. Transfer matrices are, in general, symmetric.⁹ Our approach has characteristics of both. We have set ψ in terms of a Boltzmann factor, but ϕ has the entropic prefactor. As stated in our model $K > 0$. The reason for introducing K in our system is that we believe it gives some information about the eventual barrier heights surrounding the "catchment" area of the global minimum in configuration space. Since we have referred the zero of energy to $\Delta V, K + \Delta V$ might be associated with an average potential-energy barrier outside the global minimum well. However, the cluster only sees this barrier when there is enough thermal energy to come across it. The Boltzmann factor takes account of this fact.

The values of α' were obtained from the quantities measured along one molecular-dynamics trajectory. Therefore, as shown in Fig. 6, we are comparing experi-

ment to theoretical average values. In order to check the sensitivity of the fit, we have also considered slightly different input data for f and T . For example, we have taken the f and T data reported in Tables I and II for trajectories 300, 600, and 900 τ long and recalculate α' in each case. The estimated error is 3%. The error bars for the melting temperature can be extracted from the changes of f when its value is close to $\frac{1}{2}$, which is at most 8%. Finally, the estimation of the temperature error bars is of the order of 2%, as seen in the tables.

Suppose now that ψ is not given a Boltzmann factor type of dependence, but rather is taken as $\frac{1}{4}$ for all temperatures. In that case, for the same value of α' and T_m we obtain the dashed curves of Figs. 6(a) and 6(b). It is clear that this effect is minor.

Assuming that the condition $\Delta V \gg \delta$ is fulfilled, the transition will be sharper as Ω increases. The slope of f at its half value is α/ψ . Larger cluster will show increasingly sharper transitions because Ω increases with the size of the cluster. Suppose that $\Delta V \approx \delta$ and Ω is small. In this case the transition becomes very broad. However, just for comparison, the dotted lines in Figs. 6(a) and 6(b) shows the limiting case of $\Omega = 1$. Another interesting situation can be encountered when $\Delta V \approx \delta$ and Ω is large. In this case the expansion in Eq. (10) is questionable since the first derivative is small and, therefore, higher-order terms should be included. Thus, more parameters will probably be needed in this instance.

IV. DISCUSSION

Even though we have been able to investigate only 1000 inherent configurations for each cluster size, several conclusions can be drawn. The idea of resolving observable order in a system into a structural part and a vibrational part is not new, since it underlies the study of pair correlation functions.¹² In the past⁴ we have emphasized this point and reported in molecular-dynamics studies how the pair correlation function, or the coordination number, vary with temperature during "melting." As has been pointed out by Gadzuk,²¹ and by Cotterill²² in classical trajectories, the system spends longer times at the saddle points between two minima as opposed to in the wells. Since the velocities have their lowest value at the barrier, the oscillating geometry of the cluster appears "colder" in these regions of configuration space. The measure of f is therefore not a direct measure of the fraction of time spent by the system in each well. It does, however, give an indication of where in configuration space the relevant contributions to averages might come from.

The description given in this paper relies on the knowledge of certain characteristics of the cluster configurational hypersurface, namely ΔV , δ , and the number of minima. It replaces the difficulty of performing an average over many molecular-dynamics runs starting from different initial conditions, and over variable lengths of time by a simpler dynamics—that of a correlated walk. The approach is phenomenological but instructive. It equates the structural information obtained in n snapshots along a trajectory in phase space, with a "poly-

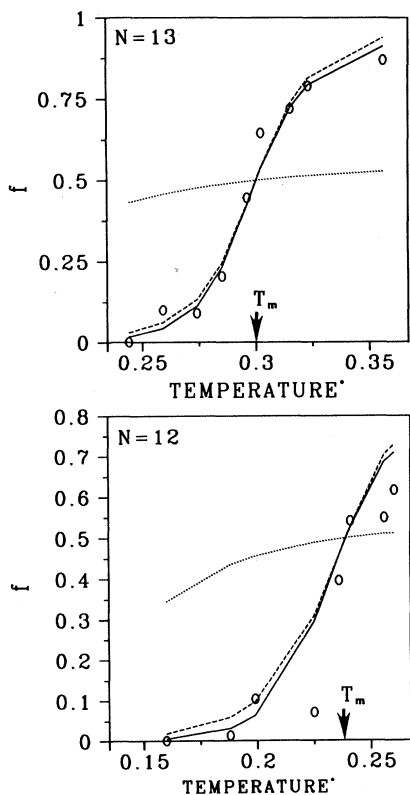


FIG. 6. Average fraction of visited minima f as a function of temperature. Solid line corresponds to Eq. (8); open circles are the experimental values given in Table I; dashed lines correspond to $\psi = \frac{1}{4}$ (temperature independent); dotted lines show the limit to the random model. Temperature is in reduced units.

mer" containing n_B broken icosahedra and $n - n_B$ intact icosahedra. In this analogy, the polymer binding term $\alpha\Delta V$ is temperature dependent. The larger this term, the sharper is the transition. This term is taking care of the contribution to the melting transition due to the region of configuration space corresponding to the minima wells. The interaction K between neighboring units in a polymer is positive. In our model K accounts for the contribution to the transition due to those regions of configurations space *outside* the catchment area of the minima. Little is known about these regions. For that reason, we have adopted a conservative approach by considering the limiting value for this energy which favors dimers. Suppose, however, that we knew more about the saddles, or other intricate paths. In that case it would be possible to change the value of K such as to favor more (or less) large sequences of B 's. We suspect that such will be the situation in large clusters. If $K > 0$, larger α values will give rise to sharper transitions.

At the beginning of the preceding section we stated that the model gives a good description of the melting process in clusters when $\Delta V \gg \delta$ and Ω is large. This set of characteristics can be used to define a class of clusters. These clusters can exhibit a melting curve such as shown in Fig. 6. However, the clusters might evaporate before melting. Clusters melt if $f > \frac{1}{2}$ before evaporation. That is the case of the 12- and 13- atom clusters. On the other hand, if $f < \frac{1}{2}$ when the evaporation threshold is reached, then the cluster never melts. Such is the case of the 14-atom cluster. Moreover, for this class of clusters the average number of contacts IB can be calculated from Eq. (6). This quantity gives an indication of the average length of the sequences having only B 's (or only I 's),

$$\frac{\langle n_{IB} \rangle}{n} = \frac{2\psi^2\phi}{\lambda_0[(1-\phi)^2 + 4\psi^2\phi]^{1/2}} \quad (12)$$

This averaged quantity has its maximum at the transition temperature: $\psi/(1+\psi)$. It is less for higher temperatures, because there are more strings having many B 's together. It is less for low temperatures, because there are no B 's in this limit. A generalization of this class of clusters can easily be included in the model. Specifically, those clusters that present a set of low-energy minima (not just one) very close together, and well detached by a gap from another set of local minima at higher potential energies. In such cases, all the low-energy minima are represented by I 's and the entropic factor ϕ_0 must be modified accordingly.

When the requirement $\Delta V \gg \delta$ is satisfied, but $\Omega \approx 1$, then the model gives rise to a broad transition. In this case we have a second class of clusters, specifically, systems presenting only one, two, or three very well-defined isomers (1, 2, or 3 minima) below the evaporation threshold. The transition is very broad in this case. These clusters behave more like molecules and therefore they can be treated as such. Temperature changes of the conformers can be understood on the basis of isomerization, hence the temperature variation of the isomer concentration is calculated directly from the change in free energy; probably very accurately in the harmonic approximation.

The extreme situation is a cluster with only one stable configuration that evaporates if enough temperature is given to it.

A third class of clusters emerges according to the previous analysis. Clusters where $\Delta V \approx \delta$ and Ω is large below the evaporation threshold. These kind of clusters are amorphouslike. The hypersurface in configuration space is shallow. Clusters belonging to this class need, of course, a much closer examination. We cannot frame them within the work presented in this paper. In this case, further neighbor interactions might be needed.

Great interest also surrounds the interpretation of magic numbers, clusters that are recorded with large abundance in mass spectrometry or photodetachment experiments. Specifically, one could seek to identify magic numbers with the realization of the class of clusters described here and a sharp change of f with temperature. If this condition is satisfied for a given N , but the cluster with $N + 1$ atoms does not melt, then N would be a magic number.

V. CONCLUSION

Previous approaches to describe melting in clusters rely on the study of the vibrations in the clusters—bimodal distribution of temperatures,² temperature dependence of the mean-square displacement,^{2,23} changes between the angle subtended in any triplet of atoms.^{4,20} Moreover, we have shown in Sec. II that Lindemann's criterion leads to very low melting temperatures. This criterion includes the assumption of harmonic motions.

In this work we have presented an alternative approach. The state of order can be associated with the number of times the cluster is found to access the global minimum of the potential energy. The state of disorder is associated with the number of times the cluster accesses all other local minima of the potential-energy hypersurface (f). Melting can be observed by following the changes with temperature between these two states. This quantity, f , presents an S -shaped behavior, defining the melting temperature T_m when its value is one-half. This is a novel criterion to locate T_m for a selected kind of clusters where $\Delta V \gg \delta$ and Ω is large.

This behavior is analogous to the melting process in a polymer undergoing the helix-coil transition or a denaturation process. The function f can be calculated within this model leading to an analytic expression. Its sigmoid shape is characteristic of a process where "cooperativity" is important. A measure of how cooperative a phenomenon can be is given by the slope of f at T_m , i.e., $\sim \alpha'/\psi$. The larger the slope, the more cooperative the process under study is. Cooperativity in this case indicates that when the cluster visits one local minimum above the gap, it is easier to access another local minimum in the next visit. The values of the parameters in this theory are given in terms of cluster quantities (ΔV , δ , Ω) and extracted from the computer experiment (T_m , α').

In summary, if the cluster is such that a gap in potential energy exists between the global and the lowest local minima of the potential energy, then f is S shaped, and melting might be observed. If the cluster does not

present a gap, then f becomes a smooth function and melting is not visible (amorphous clusters). If the cluster exhibits only a few mechanically stable isomers, changes in temperature can be described in terms of chemical equilibrium between various well defined isomers.

ACKNOWLEDGMENTS

E.B.B. thanks Professor Hans C. Andersen for very interesting comments concerning the phenomenological

model and Dr. J. W. Gadzuk and Dr. Marc Nyden for encouraging discussions. Computations were done at Centro de Investigaciones Científicas y Estudios Superiores de Ensenada. This research was partially supported by Consejo Nacional de Ciencia y Tecnología, México (PCEXCNA-050838). E.B.B. acknowledges support by the Army Research Office (DAAG 29-85-K-0244) and the hospitality of Virginia Commonwealth University.

*On sabbatical leave from Instituto de Física, Universidad Nacional Autónoma de México, Ap. Postal 20-364, México 01000 D.F., Mexico.

- ¹D. J. McGinty, *J. Chem. Phys.* **58**, 4733 (1973); W. D. Kristensen, E. J. Jensen, and R. M. J. Cotterill, *ibid.* **60**, 4161 (1974); C. L. Briant and J. J. Burton, *ibid.* **63**, 2045 (1975); R. D. Eppers and J. B. Kaelberg, *Phys. Rev. A* **11**, 1068 (1975); J. B. Kaelberer and R. D. Eppers, *J. Chem. Phys.* **66**, 3233 (1977); V. V. Nauchitel and A. J. Perstin, *Mol. Phys.* **40**, 1341 (1980); N. Quirke and P. Sheng, *Chem. Phys. Lett.* **110**, 63 (1984); R. S. Berry, J. Jellinek, and G. Natason, *Phys. Rev. A* **30**, 919 (1984).
- ²J. Jellinek, T. L. Beck, and R. S. Berry, *J. Chem. Phys.* **84**, 2783 (1986); T. L. Beck and R. S. Berry, *ibid.* **88**, 3910 (1988).
- ³J. D. Honeycutt and H. C. Andersen, *J. Phys. Chem.* **91**, 4950 (1987).
- ⁴E. Blaisten-Barojas and H. C. Andersen, *Surf. Sci.* **156**, 548 (1985); E. Blaisten-Barojas and D. Levesque, *Phys. Rev. B* **34**, 3910 (1986); E. Blaisten-Barojas, I. L. Garzon, and M. Avalos-Borja, *ibid.* **36**, 8447 (1987).
- ⁵U. Even, N. Ben-Horin, and J. Jortner, *Phys. Rev. Lett.* **62**, 140 (1989).
- ⁶B. H. Zimm and J. K. Bragg, *J. Chem. Phys.* **31**, 526 (1959); J. A. Schellman, *J. Phys. Chem.* **62**, 1485 (1958); J. H. Gibbs and E. A. DiMarzio, *J. Chem. Phys.* **30**, 271 (1959); T. L. Hill, *ibid.* **30**, 383 (1959); K. Nagai, *J. Phys. Soc. Jpn.* **15**, 407 (1960); A. Miyake, *J. Polym. Sci.* **46**, 169 (1960).
- ⁷S. Fujita, E. Blaisten-Barojas, M. Torres, and S. Godoy, *J. Chem. Phys.* **75**, 3097 (1981).

⁸For a detailed treatise containing reprints of the original contributions see, D. Poland and H. A. Scheraga, *Theory of Helix-Coil Transitions in Biopolymers* (Academic, New York, 1970).

- ⁹C. J. Thompson, *Mathematical Statistical Mechanics* (Princeton University Press, Princeton, 1972), Chap. 7.
- ¹⁰F. H. Stillinger and T. A. Weber, *Kinam* **3A**, 159 (1981); *Phys. Rev. A* **25**, 978 (1982).
- ¹¹F. A. Lindemann, *Z. Phys.* **11**, 609 (1910).
- ¹²L. Verlet, *Phys. Rev.* **165**, 201 (1968); J. P. Hansen and L. Verlet, *ibid.* **184**, 151 (1969).
- ¹³M. R. Hoare, *Adv. Chem. Phys.* **40**, 49 (1979).
- ¹⁴M. R. Hoare and J. A. McInnes, *Adv. Phys.* **32**, 791 (1983).
- ¹⁵J. A. Northby, *J. Chem. Phys.* **87**, 6166 (1987).
- ¹⁶I. Oksuz, *Surf. Sci.* **122**, L585 (1982).
- ¹⁷L. Verlet, *Phys. Rev.* **159**, 98 (1964).
- ¹⁸T. P. Martin, *Phys. Rep.* **95**, 167 (1983).
- ¹⁹I. L. Garzon and E. Blaisten-Barojas, *Chem. Phys. Lett.* **124**, 84 (1986).
- ²⁰N. Quirke, *Mol. Simul.* **1**, 207 (1988).
- ²¹J. W. Gadzuk, *J. Opt. Soc. Am. B* **4**, 201 (1987); T. S. Jones, S. Holloway, and J. W. Gadzuk, *Surf. Sci.* **184**, L421 (1987).
- ²²R. M. J. Cotterill and J. V. Madsen, *Phys. Rev. B* **33**, 262 (1986).
- ²³J. Jortner, D. Scharf, and U. Landman, in *Elemental and Molecular Clusters*, Vol. 6 of *Materials Science*, edited by G. Benedek, T. P. Martin, and G. Pacchioni (Springer-Verlag, Berlin, 1988), p. 148.